Journal of Radiation Research, 2013, 54, 70–75
doi: 10.1093/jrr/rrs079 Advance Access Publication 10 September 2012

Relative biological effects of neutron mixed-beam irradiation for boron neutron capture therapy on cell survival and DNA double-strand breaks in cultured mammalian cells

Kakuji OKUMURA[1], Yuko KINASHI[1], Yoshihisa KUBOTA[2], Erika KITAJIMA[3], Ryuichi OKAYASU[2], Koji ONO[1] and Sentaro TAKAHASHI[1,*]

[1]Research Reactor Institute, Kyoto University, Kumatori-cho, Sennann-gun, Osaka 590-0494, Japan
[2]National Institute of Radiological Sciences
[3]Osaka High-technology College
*Corresponding author. Research Reactor Institute, Kyoto University, 2-chome Asashironishi, Kumatori-cho, Sennann-gun, Osaka 590-0494, Japan. Tel: +81-724-51-2410; Fax: +81-724-51-2623; Email: sentaro@rri.kyoto-u.ac.jp

(Received 25 May 2012; revised 27 July 2012; accepted 3 August 2012)

Understanding the biological effects of neutron mixed-beam irradiation used for boron neutron capture therapy (BNCT) is important in order to improve the efficacy of the therapy and to reduce side effects. In the present study, cell viability and DNA double-strand breaks (DNA-DSBs) were examined in Chinese hamster ovary cells (CHO-K1) and their radiosensitive mutant cells (xrs5, Ku80-deficient), following neutron mixed-beam irradiation for BNCT. Cell viability was significantly impaired in the neutron irradiation groups compared to the reference gamma-ray irradiation group. The relative biological effectiveness for 10% cell survival was 3.3 and 1.2 for CHO-K1 and xrs5 cells, respectively. There were a similar number of 53BP1 foci, indicators of DNA-DSBs, in the neutron mixed-beam and the gamma-ray groups. In addition, the size of the foci did not differ between groups. However, neutron mixed-beam irradiation resulted in foci with different spatial distributions. The foci were more proximal to each other in the neutron mixed-beam groups than the gamma-ray irradiation groups. These findings suggest that neutron beams may induce another type of DNA damage, such as clustered DNA-DSBs, as has been indicated for other high-LET irradiation.

Keywords: Neutron; gamma-rays; CHO; survival; 53BP1

INTRODUCTION

Boron neutron capture therapy (BNCT) selectively destroys tumor tissue due to a $^{10}B(n,\alpha)^{7}Li$ reaction, without inducing significant damage in normal tissue. In the Kyoto University Research Reactor Institute, more than 400 cancer patients have been treated with BNCT since 1990, obtaining good results comparable with other conventional cancer therapies. The neutron beam used for BNCT is generated by a nuclear reactor and is inevitably a mixed beam that contains thermal, epithermal and fast neutrons, as well as gamma-rays. Understanding the biological effects of the mixed beam will help improve the efficiency of this therapy and reduce the side effects in normal tissue. The biological effects of neutrons have been studied with respect to DNA damage, apoptosis, chromosome aberrations, and viability [1–14], but little is known about the effects induced by a mixed beam, such as that used for BNCT.

Among biological endpoints, DNA double-strand breaks (DNA-DSBs) are important and have been frequently used in many recent studies. The numbers of foci that immunochemically stain for γ-H2AX, DNA-PKcs, 53BP1, and other DNA repair proteins have previously been shown to be related to the number of DNA-DSBs [15, 16] and to be efficient and sensitive markers for monitoring DNA-DSB induction and repair [15–21]. Some researchers have used this method to examine differences in the induction of DNA-DSB for various types of radiation, and have shown that the kinetics of the number of DNA-PKcs foci reflect that more severe DNA damage is induced by iron-particle beams than by X-rays [18]. The number of γ-H2AX foci was smaller for the proton beam than for X-rays, but

proton-induced foci disappeared at a slower rate [19]. Up till now there have been no available data on DNA-DSBs that have been assessed based on foci of repair proteins after neutron mixed-beam irradiation for BNCT. In the present study, we investigate the relative biological effectiveness (RBE) of neutron mixed-beam irradiation for BNCT using conventional cell viability and DNA-DSBs as biological endpoints.

For ionizing radiation, the RBE value increases with linear energy transfer (LET), peaks (around 100 – 200 keV/μm), and then decreases for DNA repair-proficient cells, whereas the RBE value constantly decreases with LET in repair-deficient cells [22, 23]. Neutrons with relatively high energy are classified as high-LET radiation, and it has been shown that neutrons have various high RBE values [4, 7, 10, 11]. On the other hand, some research has shown that there are low RBE values (~ 1) for neutron-induced apoptosis in human lymphocytes [9, 12]. This type of variation occurs because RBE is influenced by a range of factors, such as total dose, dose rate, irradiated cell lines, and biological endpoints, in addition to LET and energy. Although it may be difficult to estimate the precise RBE value due to these factors, understanding the biological effects and qualitative differences in the neutron mixed beam are essential for examining the efficiency and safety of BNCT. Here, we describe the RBE of the mixed-radiation beam used for BNCT at Kyoto University Research Reactor (KUR) based on the cell survival rate and DNA-DSBs.

MATERIALS AND METHODS

Cell culture

Chinese hamster ovary-derived, wild-type CHO-K1 cells were purchased from Riken BRC Cell Bank, and radiosensitive xrs5 mutant cells (Ku80-deficient cell line) were kindly supplied by Prof. P. Jeggo [24, 25]. The cells were cultured in MEMα medium (Invitrogen) supplemented with 10% heat-inactivated FBS (Biowest) and maintained at 37°C in a humidified atmosphere with 5.0% CO_2.

Irradiation

For irradiation, confluent cells were trypsinized, suspended in the above-mentioned medium, and then aliquoted into Teflon tubes. The cells were irradiated with the neutron mixed beam at the Heavy Water Facility of the Kyoto University Research Reactor (KUR) operated at 1 MW power output. Neutron fluencies and gamma-ray doses were measured based on the radioactivation of gold foil and thermoluminescent dosimeters, respectively. The physical dose rates of thermal (<0.5 eV), epithermal (0.5 – 10 keV), and fast (>10 keV) neutrons, as well as the gamma-rays in the mixed beam are summarized in Table 1. The radiation doses slightly varied with each irradiation due to the variation in the output power of the reactor and the location of the Teflon tube. For the mixed beam, approximately half of the total dose came from the gamma-rays, while the remaining half was from neutrons. Gamma-ray irradiation was performed as a control with a ^{60}Co gamma-ray irradiator at a dose rate of approximately 40 mGy/min.

Cell survival assay

The survival rates of the irradiated cells were determined using conventional colony-formation assay. After irradiation, cell suspensions were diluted, and a known quantity of cells were seeded in cell culture dishes and then incubated for 7 – 9 days. The cells were fixed with 70% ethanol and stained with crystal violet solution (Wako) in order to visualize and count the colonies.

Immunofluorescence staining

Irradiated cells were seeded onto 22 × 22 mm coverslips in 6-well microplates, incubated for 30 min or 1, 3, or 24 h, and washed with cold PBS (Invitrogen). The cells were fixed with 3.6% formalin/PBS for 10 min, permeabilized with 0.5% Triton X-100/PBS on ice for 5 min, and then washed thoroughly with PBS. The coverslips were incubated for 2 h at 37°C with a primary rabbit monoclonal anti-53BP1 antibody (Bethyl Laboratories) in TBS-DT solution (20 mM Tris-HCl and 137 mM NaCl, containing 0.1% Tween-20 and 5% skim milk). After three washes with cold PBS, the cells were incubated for 1 h at 37°C with a secondary Alexa Fluor 594 goat anti-rabbit IgG antibody (Invitrogen) in TBS-DT solution. After washing three times with PBS, the coverslips were mounted on glass slides with DAPI (4-6-diamidino-2-phenylindole) in 10% glycerol/PBS to counterstain the nuclei.

Image acquisition and analysis

Images were acquired with a fluorescence microscope (KEYENCE, BZ-9000). BZ-9000 optional software and

Table 1. Physically absorbed doses of thermal, epithermal, fast neutrons, and gamma-rays in the neutron mixed beam, when the samples were irradiated with KUR operated at 1 MW for 50 min

	Thermal neutrons (<0.5 eV)	Epithermal neutrons (0.5–10 keV)	Fast neutrons (>10 keV)	Gamma-rays	Total
Dose (Gy)	0.47 (25%) – 0.51(26%)	0.050 (2.6%) – 0.054 (2.7%)	0.34 (18%) – 0.38 (19%)	1.0 (50–53%)	1.9–2.0

The numbers in parentheses indicate the percentages of the dose relative to the total dose.

ImageJ (National Institutes of Health) were used for counting the number of foci and measuring the foci size (area). Foci number counting was carried out at magnification of × 120 and the size measurements were at × 60 and × 120.

RESULTS

Cell survival

Figure 1 shows the fraction of surviving CHO-K1 cells (referred to as K1 in Fig. 1) and xrs5 cells that had been irradiated with the neutron mixed beam or gamma-rays. A scatter plot was used because the dose rate was not available in real time, thus the total doses were not always the same for mixed-beam irradiation. Each point shows the survival fraction, and the black and dotted lines were used to fit the log-linear model with Microsoft Excel software. As expected, xrs5 cells defective in repair were more sensitive to both mixed-beam and gamma-ray irradiation than CHO-K1 cells. Mixed-beam irradiation seems to be more effective in CHO-K1 cells, and slightly more effective in xrs5 cells, compared with control ^{60}Co gamma-ray irradiation. Although the doses were available below 2.6 Gy, extrapolation of the best-fit line indicated that the RBE for 10% survival is 3.3 and 1.2 for CHO-K1 and xrs5 cells, respectively.

The number of 53BP1 foci

Figure 2 shows the number of 53BP1 foci in CHO-K1 and xrs5 cells at 1 h after irradiation. The number of 53BP1 foci per cell in both cell lines increased linearly with the radiation dose up to 0.5 – 1 Gy, and then the rate of increase appeared to decrease. There were no significant differences in the number of foci between cells irradiated with the mixed beam and gamma-rays.

Figure 3 shows the time-dependent disappearance of 53BP1 foci following 1 Gy of neutron mixed-beam or gamma-ray irradiation. The number of 53BP1 foci was significantly higher in xrs5 cells than in CHO-K1 cells for both mixed-beam and gamma-ray irradiation. This result is consistent with the finding that xrs5 cells are more sensitive to neutrons and gamma-rays, as shown in Fig. 1. The number of 53BP1 foci for xrs5 cells at 3 h after irradiation did not substantially decrease, and remained high compared with CHO-K1 cells. This is because DNA-DSB repair in CHO-K1 cells is efficient regardless of the radiation type.

Size and spatial distribution of foci

The focus size was measured using two different methods. In the first method, the magnification was set to × 60, the

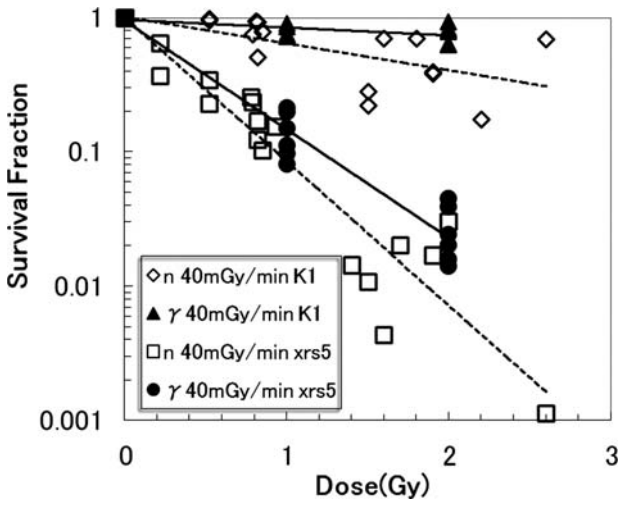

Fig. 1. Comparison of the surviving fraction for neutron mixed beam (n) and gamma-rays (γ) at 40 mGy/min. Each point shows the survival fraction; the black and dotted lines were used to fit the log-linear model with Microsoft Excel software. The neutron mixed beam is more effective than the gamma-rays. The xrs5 cells were more sensitive than CHO-K1 cells to both kinds of radiation.

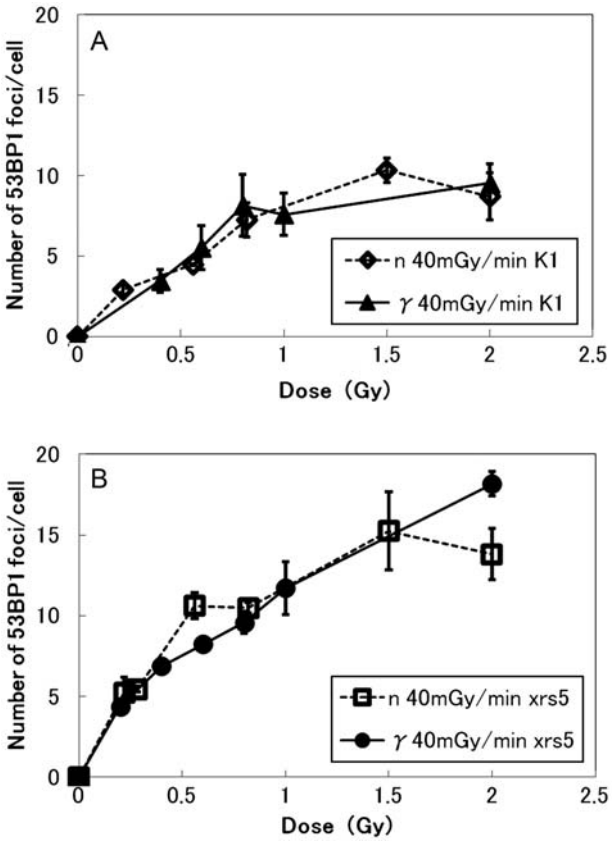

Fig. 2. The number of 53BP1 foci 1 h after irradiation. The data were compiled from two or three independent experiments. The error bars indicate the standard errors of the mean. Panel A: 53BP1 foci in CHO-K1 cells. Panel B: 53BP1 foci in xrs5 cells. The number of 53BP1 foci per cell in both cell lines increased linearly with the radiation dose up to 0.5 – 1 Gy, and then the rate of increase decreased.

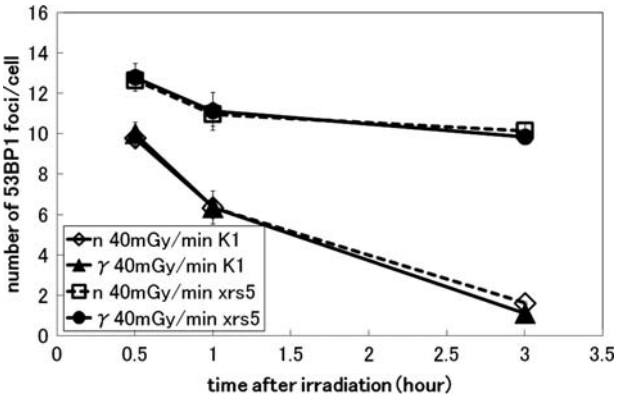

Fig. 3. Induction and disappearance of 53BP1 foci in CHO-K1 cells and xrs5 cells 3 h after 1 Gy of neutron mixed beam or gamma-rays. The number of 53BP1 foci was significantly higher in xrs5 cells than in CHO-K1 cells for both mixed-beam and gamma-ray irradiation.

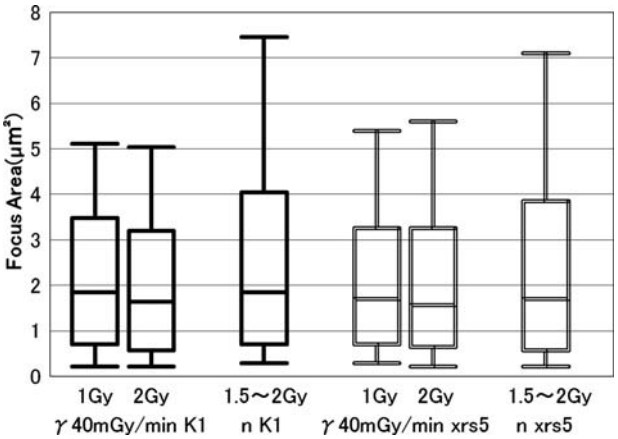

Fig. 4. Comparison of the 53BP1 focus size observed at ×60 magnification 1 h post gamma-ray (γ) or neutron mixed-beam (n) irradiation. The area of 53BP1 foci was measured with KEYENCE BZ-9000 optional software using settings in which the image brightness and contrast were optimized for visual counting. Box and whisker plot: whiskers indicate the range between the 10th and 90th percentiles; boxes represent the distance between the first and third quartiles and the median between them.

brightness and contrast were optimized for visual observation, and the focus area was determined using KEYENCE BZ-9000 optional software. As shown in Fig. 4, the median size did not differ between the neutron mixed beam and gamma-rays, but the size distribution tended to be larger with neutron mixed-beam irradiation. We noticed that under these conditions some foci could not be counted separately, and a few of the small foci were counted as one aggregated focus. Many more foci were located close to each other in the neutron mixed-beam irradiation than in the gamma-ray group. This is because the focus size was measured as larger in the neutron mixed-beam group (as

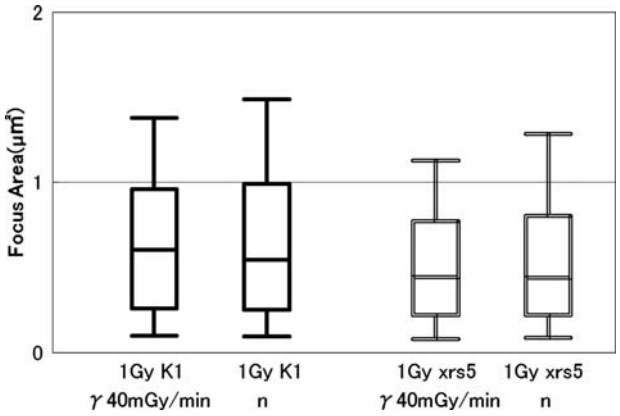

Fig. 5. Comparison of 53BP1 focus size observed at ×120 magnification 1 h post gamma-ray (γ), or neutron mixed-beam (n) irradiation. The areas of 53BP1 foci were measured using ImageJ, in which the image brightness and contrast were optimized for automatic counting. Box and whisker plot: whiskers indicate the range between the 10th and 90th percentiles; boxes represent the distance between the first and third quartiles and the median between them.

shown in Fig. 4). With the second area measurement technique, the magnification was set to × 120 to detect smaller foci, and the image brightness and contrast were optimized for automatic counting by ImageJ. This time the smaller foci, which were difficult to detect separately using the first measurement setting, were included in the analysis, making the median focus size much smaller compared with those in Fig. 4. There were no significant differences in the median focus size or in the 90% values when comparing the neutron and gamma-ray irradiation (Fig. 5).

DISCUSSION

Previous reports showed that RBE values for neutrons were relatively high depending on the energy. The RBE values are at a maximum at 0.3 – 0.4 MeV neutrons, and then decrease as the energy increases; they also decline at <0.3 MeV neutrons [11, 26]. The neutron mixed beam used here includes approximately 25% thermal (<0.5 eV) neutrons and 20% fast (>10 keV) neutrons that contribute to the total physical dose. Therefore, it is difficult to determine the exact RBE value for each range of neutron energy. Our work showed that the RBE for the neutron mixed beam at 10% survival dose (D10) was 3.3 and 1.2 for CHO-K1 and xrs5 cells, respectively. The RBE for xrs5 cells is consistent with previously reported RBE values [18, 23].

DNA-DSBs are the most hazardous lesions in cells. High-LET radiation induces DNA-DSBs that are not repaired or are more difficult to repair compared to low-LET radiation [18, 27, 28]. DNA-DSBs are repaired by homologous recombination (HR) or non-homologous end

joining (NHEJ), and xrs5 cells are deficient in NHEJ [29]. The number of 53BP1 foci was larger in xrs5 cells than CHO-K1 cells for both mixed-beam and gamma-ray irradiation (Fig. 3). These data and Fig. 1 suggest that xrs5 cells show high radiosensitivity to neutrons, as was previously demonstrated in studies using gamma-rays, X-rays or heavy ion irradiation [24, 25, 29, 30]. The number of DNA-DSBs induced by the neutron mixed beam and by gamma-rays was similar: Fig. 2 and Fig. 3 do not show much difference between neutrons and gamma-rays.

In the present paper, we have only shown the data on the foci of 53BP1. A similar tendency was also obtained for γH2AX foci, but the data are not shown here. It is known that both γH2AX and 53BP1 can detect DNA-DSBs sensitively, and there are essentially no differences in the detection sensitivity between them. Therefore, the kinetics of focus formation observed here may represent the kinetics of DNA-DSBs in general.

At the low magnification (× 60), the sizes of foci were larger in cells irradiated with neutron beams (Fig 4). This is because the low magnification could not clearly resolve the images of each focus. It seems that the results with higher magnification (× 120) in Fig. 5 show more accurate foci size distribution, and there were no differences in the size of each focus induced by the neutron mixed beam or gamma-rays. However, as indicated in Fig. 4, it also appears that the DNA-DSBs induced by the mixed beam may be clustered because neutrons have high LET values [31]. These findings may indicate that neutrons induce different types of DNA-DSBs such as clustered DNA-DSBs, although the number of DNA-DSBs and the focus size are similar to those induced by low-LET gamma-rays.

In this study, we used a colony formation assay to compare the biological effectiveness of neutron mixed-beam irradiation and gamma-ray irradiation in CHO-K1 and xrs5 cells, and found significant differences between them. However, the number of 53BP1 foci and the size of each focus does not appear to differ between the neutron beam and gamma-rays. The kinetics of the number of 53BP1 foci following 1 Gy irradiation (i.e. focus disappearance) was also similar between these types of radiation. The only noted difference was the spatial distribution of the foci. The foci were located more proximally to each other in the neutron mixed-beam than the gamma-ray irradiation groups. Although xrs5 cells had a lower survival rate and greater number of 53BP1 foci compared to CHO-K1 cells, the size distributions of foci were found to be the same in these two cell lines.

FUNDING

This work was supported by the Nuclear Safety Promotion Research Program, Cabinet Office, Japan, and was partially supported by the NIRS International Open laboratory (IOL) and the Chang Yung-Fa Foundation.

ACKNOWLEDGEMENTS

We thank Yoshinori Sakurai and Hiroki Tanaka for technical assistance with radiation dose measurements. We greatly appreciate Chris Allen's assistance in the form of English proof-reading.

REFERENCES

1. Bauchinger M, Koester L, Schmid E *et al*. Chromosome aberrations in human lymphocytes induced by fission neutrons. *Int J Radiat Biol* 1984;**45**:449–57.
2. Goodhead DT. Initial events in the cellular effects of ionizing radiations: clustered damage in DNA. *Int J Radiat Biol* 1994;**65**:7–17.
3. Peak MJ, Wang L, Hill CK *et al*. Comparison of repair of DNA double-strand breaks caused by neutron or gamma radiation in cultured human cells. *Int J Radiat Biol* 1991;**60**:891–8.
4. Hendry JH, Potten CS, Merritt A. Apoptosis induced by high- and low-LET radiations. *Radiat Environ Biophys* 1995;**34**:59–62.
5. Schmid E, Regulla D, Guldbakke S *et al*. The effectiveness of monoenergetic neutrons at 565 keV in producing dicentric chromosomes in human lymphocytes at low doses. *Radiat Res* 2000;**154**:307–12.
6. Schmid E, Regulla D, Guldbakke S *et al*. Relative biological effectiveness of 144 keV neutrons in producing dicentric chromosomes in human lymphocytes compared with 60Co gamma rays under head-to-head conditions. *Radiat Res* 2002;**157**:453–60.
7. Schmid E, Schlegel D, Guldbakke S *et al*. RBE of nearly monoenergetic neutrons at energies of 36 keV-14.6 MeV for induction of dicentrics in human lymphocytes. *Radiat Environ Biophys* 2003;**42**:87–94.
8. Vral A, Verhaegen F, Thierens H *et al*. Micronuclei induced by fast neutrons versus 60Co gamma-rays in human peripheral blood lymphocytes. *Int J Radiat Biol* 1994;**65**:321–8.
9. Vral A, Cornelissen M, Thierens H *et al*. Apoptosis induced by fast neutrons versus 60Co gamma-rays in human peripheral blood lymphocytes. *Int J Radiat Biol* 1998;**73**:289–95.
10. Warenius HM, Down JD. RBE of fast neutrons for apoptosis in mouse thymocytes. *Int J Radiat Biol* 1995;**68**:625–9.
11. Tanaka K., Gajendiran N, Endo S *et al*. Neutron energy-dependent initial DNA damage and chromosomal exchange. *J Radiat Res* 1999;**40** Suppl:36–44.
12. Ryan LA, Wilkins RC, McFarlane NM *et al*. Relative biological effectiveness of 280 keV neutrons for apoptosis in human lymphocytes. *Health Phys* 2006;**91**:68–75.
13. Suda M, Hagihara T, Suya N *et al*. Specifications of a neutron exposure accelerator system for biological effects experiments (NASBEE) in NIRS. *Radiat Phys Chem* 2009;**78**:1216–9.
14. Vandersickel V, Mancin M, Slabbert J *et al*. The radiosensitizing effect of Ku70/80 knockdown in MCF10A cells

irradiated with X-rays and p(66)+Be(40) neutrons. *Radiat Oncol* 2010;**5**:30.
15. Kinner A, Wu W, Staudt C *et al*. Gamma-H2AX in recognition and signaling of DNA double-strand breaks in the context of chromatin. *Nucleic Acids Res* 2008;**36**:5678–94.
16. Chan DW, Chen BPC, Prithivirajsingh S *et al*. Autophosphorylation of the DNA-dependent protein kinase catalytic subunit is required for rejoining of DNA double-strand breaks. *Genes Dev* 2002;**16**:2333–8.
17. Hidaka M, Oda S, Kuwahara Y *et al*. Cell lines derived from a Medaka radiation-sensitive mutant have defects in DNA double-strand break responses. *J Radiat Res* 2010;**51**:165–71.
18. Okayasu R, Okada M, Okabe A *et al*. Repair of DNA damage induced by accelerated heavy ions in mammalian cells proficient and deficient in the non-homologous end-joining pathway. *Radiat Res* 2006;**165**:59–67.
19. Antoccia A, Sgura A, Berardinelli F *et al*. Cell cycle perturbations and genotoxic effects in human primary fibroblasts induced by low-energy protons and X/γ-rays. *J Radiat Res* 2009;**50**:457–68.
20. Okada T, Kashino G, Nishiura H *et al*. Micronuclei formation induced by X-ray irradiation does not always result from DNA double-strand breaks. *J Radiat Res* 2012;**53**:93–100.
21. Kitajima S, Nakamura H, Adachi M *et al*. AT Cells show dissimilar hypersensitivity to heavy-ion and X-rays irradiation. *J Radiat Res* 2010;**51**:251–5.
22. Lett JT, Cox AB, Bergtold DS. Cellular and tissue responses to heavy ions: basic considerations. *Radiat Environ Biophys* 1986;**25**:1–12.
23. Weyrather WK, Ritter S, Scholz M *et al*. RBE for carbon track-segment irradiation in cell lines of differing repair capacity. *Int J Radiat Biol* 1999;**75**:1357–64.
24. Jeggo PA, Kemp LM. X-ray-sensitive mutants of Chinese hamster ovary cell line. Isolation and cross-sensitivity to other DNA-damaging agents. *Mutat Res* 1983;**112**:313–27.
25. Kemp LM, Sedgwick SG, Jeggo PA. X-ray sensitive mutants of Chinese hamster ovary cells defective in double-strand break rejoining. *Mutat Res* 1984;**132**:189–96.
26. Hopewell JW, Morris GM, Schwint A *et al*. The radiobiological principles of boron neutron capture therapy: a critical review. *Appl Radiat Isot* 2011;**69**:1756–9.
27. Hill MA. Radiation damage to DNA: The importance of track structure. *Radiat Meas* 1999;**31**:15–23.
28. Terato H, Tanaka R, Nakaarai Y *et al*. Quantitative analysis of isolated and clustered DNA damage induced by gamma-rays, carbon ion beams, and iron ion beams. *J Radiat Res* 2008;**49**:133–46.
29. Singleton BK, Priestley A, Steingrimsdottir H *et al*. Molecular and biochemical characterization of xrs mutants defective in Ku80. *Mol Cell Biol* 1997;**17**:1264–73.
30. Ritter S, Durante M. Heavy-ion induced chromosomal aberrations: a review. *Mutat Res* 2010;**701**:38–46.
31. Hada M, Georgakilas AG. Formation of clustered DNA damage after high-LET irradiation: a review. *J Radiat Res* 2008;**49**:203–10.